M. Larakeb[1,2]
A. Bentounsi[1],
H.Djeghloud[2,*]

J. Electrical Systems 12-4 (2016): 770-785

Journal of Electrical Systems

Regular paper

On-Line Parameters Estimation of Low Scale SPSG Using Discrete Kalman Filters

Parametric identification techniques are applied in year's space from in appliances based on electrical machines. Many of these techniques are verging on each other in this field. In fact, certain techniques are more adapted to a recorded time parametric identification and which are called 'off-line methods'. The off-line methods are principally based on standstill tests. The other techniques are more suitable for a real time estimation of the parameters and are known as 'on-line methods'. The on-line methods concern mainly the case where the machine is functioning under load conditions, but both methods (off-line and on-line) may use an optimization algorithm to minimize the error between the real and the estimated parameters. In this article, the study was carried out on a salient-pole synchronous generator (SPSG) of 0.3 KW. At first, the performance of experimental parametric identification using off-line tests is presented; subsequently, different estimators were applied to on-line parametric identification. The discrete Kalman filter (DKF) is the estimator applied in this work, and it can be used in its traditional form (DTKF) for linear systems or in its extended form (DEKF) when the system is nonlinear. Another attractive application of the DKF is when it is biased (DBEKF). The consideration of the bias makes it possible to reduce the mean squared error (MSE) between measured and estimated values of the system state variable; accordingly, the normalized MSE (NMSE) can be minimized. Likewise, standard deviation (STD) between real and estimated values of the parameter can be limited in the tolerable percentage. All this study is discussed and the different DKFs are implemented in Matlab/Simulink code in order to demonstrate the effectiveness of DBEKF estimator compared to the other filters. The simulation results are satisfying since good agreement between real and estimated parameters was obtained which means an acceptable noise filtering quality of the designed Kalman estimators. All estimators can be used in on-line estimation in both steady and transient states for low scale generator.

Keywords: Kalman filter; on-line parametric estimation; bias; SPSG; NMSE.

Article history: Received 24 September 2016, Accepted 22 November 2016

1. 1.Introduction

The stability analysis of power systems requires an accurate knowledge of parameters [1,2]. Mainly synchronous machines which parameters are strongly dependent on saturation, magnetic field distribution and rotor speed [3]. Several methods were investigated for identifying synchronous machine parameters. These methods can be categorized into two big classifications: off-line methods and on-line methods. The off-line method consists of studying standstill frequency domain [4-6], time domain [7, 8], or both domains responses [9]. The profits of these off-line methods are mostly the uncomplicated testing procedures without any coupling between d and q axis. Nevertheless, the identified parameters can fail to characterize correctly the machine behaviour under various load conditions [3].

The on-line methods estimate the synchronous machines parameters on the basis of the operating data without necessitating any service interruption and costly testing. Moreover,

* Corresponding author: H. Djeghloud, University of Constantine 1, LGEC lab, Constantine, Algeria, E-mail: hind.djeghloud@umc.edu.dz
[1]University of Constantine 1, LGEC lab, Constantine, Algeria, E-mail: a.bentounsi@umc.edu.dz
[2]University of Constantine 1, LGEC lab, Constantine, Algeria, E-mail: larakeb_maria@yahoo.fr

the effects of saturation and eddy currents are automatically taken into account [2,3,10]. Furthermore, these methods have proven to be suitable for large synchronous machines under different loading levels. Likewise, the on-line estimative methods can be used for detecting some functional faults [11].

Fig.1. Photo of the considered SPSG.

However, different estimators are available for on-line parametric identification; the Discrete Kalman Filter (DKF) is one of them. The KF is the best minimum-variance state estimator for noised linear dynamic systems [12,13]. The concept of Kalman filtering consists of the estimate state of a dynamic system from partial and noised observations. For nonlinear systems, the KF remains worthwhile but modifications must first be done. These modifications comprise the extended EKF [14], the unscented KF [15,16], and the particle KF [17]. The consideration of the bias is very beneficial since it reduces the MSE [18]. The application of the KF to estimate system parameters involves establishing the mathematical model of the system dynamics from the experimental data. Digital systems have some significant benefits compared with analogue ones (or continuous-time systems) as demonstrated in many references, especially when it's a matter of the discrete extended KF (DEKF) [19-21]. Indeed, they are more repeatable, less disturbed by external conditions, have better resistance to noise, and in most modern designs they are, at least to some extent, programmable which allow modification in software instead of in hardware [22].

This work consists of applying the studies performed in [23, 24] on a very low scale SPSG (0.3 kW LEYBOLD 73236) as real values were extracted in the laboratory from standstill time domain in off-line tests [25]. The originality of our work lies in the implementation of a biased DBEKF estimator which has enabled an efficient on-line identification of the parameters of a low-power salient-pole synchronous machine. Another contribution in this area is the development of an experimental bench using a DSPACE 1104 chip board interface which allowed validating the results of different simulations carried out under Matlab/Simulink.

2. 2.Notation

V_n, I_n, f_n	nominal voltage, current and frequency of the considered SPSG.
v_d, v_q, E_f	armature direct and quadrature voltages, field (excitation) voltage.
i_d,i_q,i_f,i_{kd},i_{kq}	armature direct and quadrature currents, field current, direct and quadrature damper currents

r_a, r_f, r_{kd}, r_{kq}	resistances of armature, field, direct and quadratic dampers.
l_a, l_f, l_{kd}, l_{kq}	leakage inductances of armature, field, direct and quadratic dampers.
$L_d, L_q, L_f, L_{kd}, L_{kq}$	linkage inductances of armature, field, direct and quadratic dampers
L_{md}, L_{mq}	d-axis and q-axis magnetizing inductances
$\phi_d, \phi_q, \phi_f, \phi_{kd}, \phi_{kq}$	linkage flux of respectively armature direct and quadrature axis, field circuit, direct and quadrature dampers
ω_s, ω_b	synchronous speed and base value of the angular frequency
$X_d, X_q, X_{md}, X_{mq}, X_f, X_{kd}, X_{kq}$	d-q axis, magnetizing d-q axis, field and direct-quadratic dampers reactance's
J, F, Ω_m	inertia, friction coefficient and mechanical velocity
T_e, T_m, T_s	electrical, mechanical torques and sample time
Z_1, Z_2	the feeder impedances
A, B, C, D	matrices of state transition continuous, input, output, feed through
$x(k), u(k), y(k)$	state vector, input vector, output vector
α, z, σ	vector of parameters, extended state variable and vector of parameters to be estimated
A_d, B_d, C_d, D_d, I	discrete matrices (state transition, input, output, feed through) and the identity matrix
w, w_d, Q, Q_d	continuous/discrete state noise and their covariance matrices
v, v_d, R, R_d	continuous/discrete measurement noise and their covariance matrices

3. 3. Off-line Parametric Identification

The different experimental tests performed for parametric identification of the SPSG (Fig.1) are mainly based on the off-line methods recommended by IEC 60034-4 [9]. Table 1 indicates the specifications of the considered SPSG.

Table 1: Specifications of the considered SPSG

Power (W)	Voltage (V)	Current (A)	Frequency (Hz)	Speed (rpm)	cosφ
300	230/400 140	0.67/0.43 0.55	50	1500	1/0.8

As illustrated in the chart of Fig.1, the parametric estimation of the considered SPSG concerns electrical and mechanical parameters. Electrical parameters are resistances and inductances, while mechanical parameters are the inertia and the friction coefficient. Generally, volt-am meter method is adopted for resistances measurement and the core losses resistance can be obtained from a no-load test; the Poitier diagram method is used for the determination of armature, field leakage-inductances and d-q axis magnetizing inductances; as resistances dampers cannot be determined directly, then they can be obtained analytically from the sudden three phase short-circuit test as well as dampers leakage inductances. The mechanical parameters can be evaluated from the deceleration method or from the material point method [25].

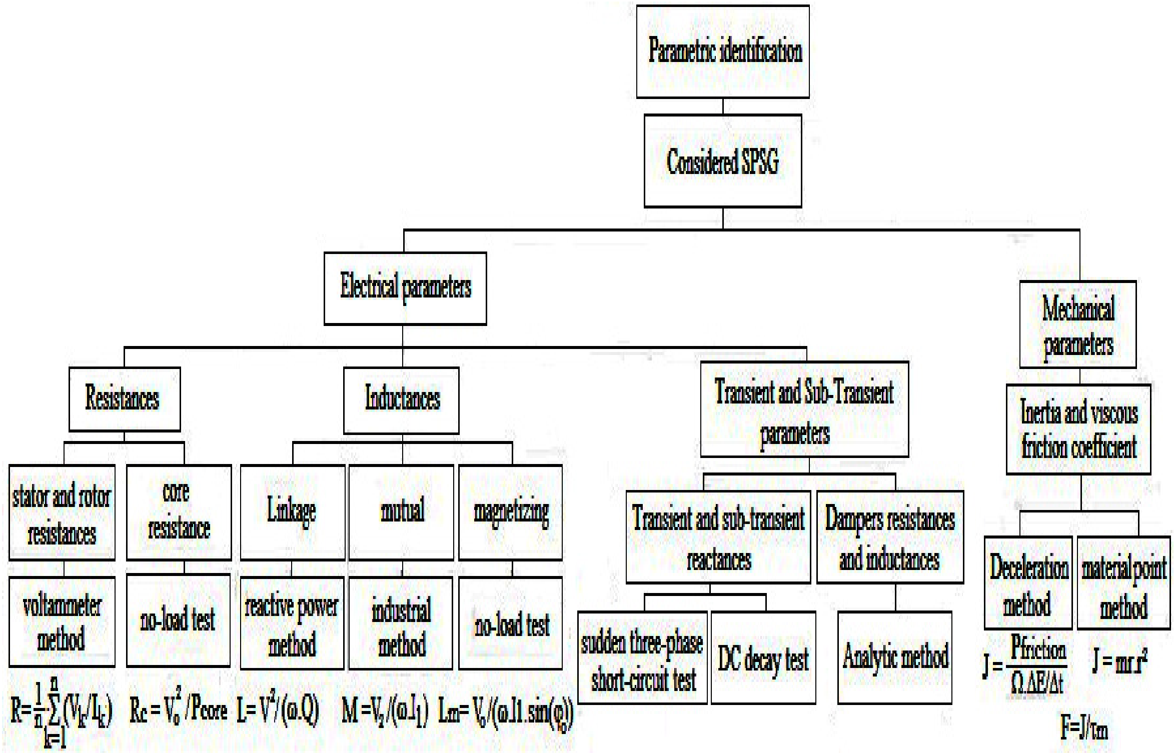

Fig.2. Off-line parameters identification method of considered SPSG.

The parametric identification of the considered SPSG was carried out following the methods given in the flow chart of Fig. 2 [25, 26]. The obtained parameters are shown in Table 2. The identified parameters are transformed into p.u system according to the methods mentioned in Table 3 [27].

Table 2: Identified parameters of the considered SPSG.

Parameters		*Method*	*Value*
Electric	Armature and field resistances	Volt-am-meter	$r_a = 41.647\ \Omega$ $r_f = 223.77\ \Omega$
	Core losses resistance	No-load test	$r_c = 9.14\ k\Omega$
	Armature and field leakage inductance	Potier diagram	$l_a = 0.2401$ H $l_f = 0.149$ H
	Direct and quadratic linkage inductances	Low slip test	$L_d = 2.30$ H $L_q = 1.37$ H
	d-q axis magnetizing inductances	Potier diagram	$L_{md} = 2.06$ H $L_{mq} = 1.13$ H
	Dampers resistances	sudden three-phase short-circuit test	$r_{kd} = 23.5\ \Omega$ $r_{kq} = 45.92\ \Omega$
	Dampers leakage inductance		$l_{kd} = 0.2401$ H $l_{kq} = 0.140$ H
Mechanical	Inertia and friction	Material point and deceleration methods	$J = 2.7\ 10^{-4}\ Kg.m^2$ $F = 13.5\ 10^{-4}$ Nm.rd/s

Table 3: Base values of armature and field of the considered SPSG

Base angular frequency		$\boldsymbol{\omega_n = \omega_{base} = 2.\pi.f_n}$
Base speed		$\Omega_{base} = \frac{\omega_{base}}{p}$
Base torque		$T_{base} = \frac{P_{a\_base}}{\Omega_{base}}$
Base power		$P_{base} = 3.V_n.I_n$
Armature /field base values		
Base voltage	$V_{a\_base} = \sqrt{2}.V_n$	$E_{f\_base} = \frac{P_{base}}{i_{f\_base}}$
Base current	$i_{a_{base}} = \sqrt{2}.i_n$	$i_{f\_base} = i_{f_n}.L_{md\_pu}$
Base impedance	$Z_{a\_base} = \frac{V_{a\_base}}{i_{a\_base}}$	$Z_{f\_base} = \frac{E_{f\_base}}{i_{f\_base}}$
Base inductance	$L_{a\_base} = \frac{Z_{a\_base}}{\omega_n}$	$L_{f\_base} = \frac{Z_{f\_base}}{\omega_n}$
d axis magnetizing inductance p.u value		$L_{md\_pu} = \frac{L_{md}}{L_{a\_base}}$
Parameters expressions in p.u system		
Value parameter		$\frac{quantity\ expressed\ in\ SI\ unit}{base\ value}$
Inertia constant H		$\frac{\frac{1}{2}.J.\Omega_{base}^2}{P_{base}}$
Friction coefficient		$\frac{T_{base}}{\Omega_{base}}$

The parameters values in p.u identified by off-line methods are grouped in Table 4.

Table 4: Real SPSG parameters values in per units

Parameter	***p. u. value***	***Parameter***	***p. u. value***
E_f	0.350	l_{kd}	0.2026
L_{md}	1.3509	l_{kq}	0.2471
L_{mq}	0.6637	p	2
r_a	0.0779	H	0.1123
r_f	0.3340	D	0.0120
l_a	0.2937	P_m	0.3
l_f	0.0699	Feeder voltage	1
r_{kd}	0.0351	$z1$	0.183+j×0.44
r_{kq}	0.0685	$z2$	0.103+j×0.44

4. On-line estimation

The on-line estimation requires the accurate choice of the machine mathematical model. Besides, it involves the implementation of an estimator. The mathematical model is generally presented in the state space form. The implementation of an estimator necessitates the consideration of state and measurement noises to be filtered by the estimator, in order to achieve good estimated parameters close to the real one.

4.1. State Space model of the SPSG

4.1.1 Nonlinear Model of the SPSG

Fig.3 portrays the d-q axis equivalent circuit of the considered SPSG; in this study the configuration of one damper on each axis was adopted. The machine equations are deduced from the models presented in [28,29]. The SPSG mathematical model is given by (1)-(11).

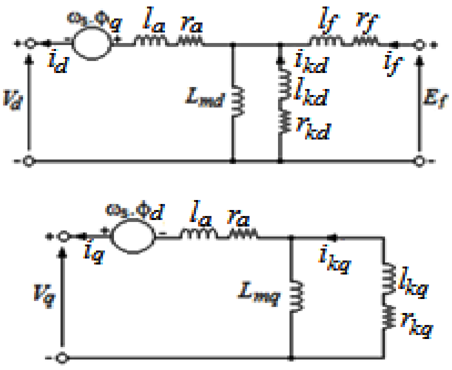

Fig.3. SPSG (a) d-axis equivalent circuit(b) q-axis equivalent circuit

$$V_d = -r_a i_d + \frac{1}{\omega_b}\frac{d\phi_d}{dt} + \omega_s \phi_q \tag{1}$$

$$V_q = -r_a i_q + \frac{1}{\omega_b}\frac{d\phi_q}{dt} - \omega_s \phi_d \tag{2}$$

$$E_f = r_f i_f + \frac{1}{\omega_b}\frac{d\phi_f}{dt} \tag{3}$$

$$0 = r_{kd} i_{kd} + \frac{1}{\omega_b}\frac{d\phi_{kd}}{dt} \tag{4}$$

$$0 = r_{kq} i_{kq} + \frac{1}{\omega_b}\frac{d\phi_{kq}}{dt} \tag{5}$$

$$\phi_d = -L_d i_d + L_{md} i_{kd} + L_{md} i_f \tag{6}$$

$$\phi_q = -L_q i_q + L_{mq} i_{kq} \tag{7}$$

$$\phi_f = -L_{md} i_d + L_{md} i_{kd} + L_f i_f \tag{8}$$

$$\phi_{kd} = -L_{md} i_d + L_{kd} i_{kd} + L_{md} i_f \tag{9}$$

$$\phi_{kq} = -L_{mq} i_q + L_{kq} i_{kd} \tag{10}$$

$$J\frac{d\Omega_m}{dt} = T_e - T_m - F.\Omega_m \tag{11}$$

4.1.2 The linearization using the state space representation

In order to apply the different DKF cited in the abstract, the set of equations from (1) to (10) has to be linearized at first. To achieve this condition, the continuous state space representation must be used as formulated in (12).

$$\begin{cases}\dot{x} = A(\alpha).x + B(\alpha).u = f(\alpha, x, u) \\ y = C(\alpha).x + D(\alpha).u = h(\alpha, x, u)\end{cases} \tag{12}$$

$A \in \mathbb{R}^{N\times N}$, $B \in \mathbb{R}^{N\times L}$, $C \in \mathbb{R}^{M\times N}$, $D \in \mathbb{R}^{M\times L}$

The N, L and M are the dimensions of the vectors describing the state, input and output, respectively,

$\alpha = [r_a\ r_f\ r_{kd}\ r_{kq}\ l_a\ l_f\ l_{kd}\ l_{kq}\ L_{md}\ L_{mq}\ \omega_b]^t$

$x = [\phi_d\ \phi_f\ \phi_{kd}\ \phi_q\ \phi_{kq}]^t$,

$u = [V_d\ E_f\ V_q]^t$,

$y = [i_d\ i_f\ i_q]^t$.

The linearization representation yields to:

$$A(\alpha) = -\omega_b.(r.\ C(\alpha) + A_1) \tag{13}$$

Where

$$r = \begin{bmatrix} -r_a & 0 & 0 & 0 & 0 \\ 0 & r_f & 0 & 0 & 0 \\ 0 & 0 & r_k & 0 & 0 \\ 0 & 0 & 0 & -r_a & 0 \\ 0 & 0 & 0 & 0 & r_{kq} \end{bmatrix}, \qquad A_1 = \begin{bmatrix} 0 & 0 & 0 & 1 & 0 \\ 0 & 0 & 0 & 0 & 0 \\ 0 & 0 & 0 & 0 & 0 \\ -1 & 0 & 0 & 0 & 0 \\ 0 & 0 & 0 & 0 & 0 \end{bmatrix},$$

$$C(\alpha) = \begin{bmatrix} \frac{-(X_f.X_{kd} - X_{md}{}^2)}{K_1} & \frac{X_{md}.(X_{kd} - X_{md})}{K_1} & \frac{X_{md}.(X_f - X_{md})}{K_1} & 0 & 0 \\ \frac{X_{md}.(X_{kd} - X_{md})}{K_1} & \frac{-(X_f.X_{kd} - X_{md}{}^2)}{K_1} & \frac{X_{md}.(X_{kd} - X_{md})}{K_1} & 0 & 0 \\ 0 & 0 & 0 & 0 & 0 \\ 0 & \frac{X_{md}.(X_{kd} - X_{md})}{K_1} & 0 & \frac{X_{kq}}{K_2} & \frac{-X_{mq}}{K_2} \\ 0 & 0 & 0 & 0 & 0 \end{bmatrix}$$

$$K_1 = X_d.X_{md}^2 + X_f.X_{md}^2 + X_{kd}.X_{md}^2 - 2.X_{md}^3 - X_d.X_f.X_{kd} \ ;\ K_2 = X_{kq}.X_q - X_{mq}^2 \tag{14}$$

$$B(\alpha) = \begin{bmatrix} \omega_b & 0 & 0 & 0 & 0 \\ 0 & \omega_b & 0 & 0 & 0 \\ 0 & 0 & 0 & 0 & 0 \\ 0 & 0 & 0 & \omega_b & 0 \\ 0 & 0 & 0 & 0 & 0 \end{bmatrix}, \qquad D(\alpha) = \begin{bmatrix} 0 & 0 & 0 & 0 & 0 \\ 0 & 0 & 0 & 0 & 0 \\ 0 & 0 & 0 & 0 & 0 \\ 0 & 0 & 0 & 0 & 0 \\ 0 & 0 & 0 & 0 & 0 \end{bmatrix}$$

4.1.3 Discrete-Time state space representation of SPSG

According to [29,30] the passage from a continuous-time system to a discrete-time system utilizing a state space representation can be done using the following paths:

$$\begin{cases} x(k+1) = A_d(\alpha).x(k) + B_d(\alpha).u(k) = F_d(\alpha, x, u) \\ y(k) = C_d(\alpha).x(k) + D(\alpha).u(k) = H_d(\alpha, x, u)\end{cases} \tag{17}$$

Where

$$A_d(\alpha) = e^{A(\alpha)T_s} \approx I_n + \frac{AT_s}{1!} + \frac{AT_s{}^2}{2!} \tag{18}$$
$$B_d(\alpha) = \int_0^{T_s} e^{AT_s} B dt \approx T_s B(\alpha) \tag{19}$$
$$C_d(\alpha) = C(\alpha)\,,\, D_d(\alpha) = D(\alpha) \tag{20}$$

5. System overview and application of the DKF estimator

Fig 4 shows how to perform an on-line estimation by applying the DKF. In this work, the machine is connected to an infinite bus represented by a feeder with a varying impedance (from z1 to z2) which allows also to provoke the transient state; the infinite bus feeder was chosen to withstand with the machine perturbations. In this study, the vector of parameters to be estimated is noted σ so that σ= [r_f, L_{md}, L_{mq}, l_{kd}, l_{kq}]. It is obvious that some of these parameters are more influent in the steady state (r_f, L_{md}, L_{mq}); whereas, the others intervene only during the transient state (l_{kd}, l_{kq}).

5.1. Principle of introduction of the DKF

The application of the DKF involves adding noises in (17). Then the system becomes stochastic since it puts into account the noise effect which is a random perturbation. Then, (17) enhances to:

$$\begin{cases} x(k+1) = A_d(\alpha).x(k) + B_d(\alpha).u(k) + I.w_d(k) \\ y(k) = C_d(\alpha).x(k) + v_d(k) \end{cases} \tag{21}$$

Where w_d and v_d are centered Gaussian pseudo-white noises with a respective covariance matrices Q_d and R_d so that the latter is invertible [31].

$$Q_d = \int_0^{T_s} e^{A.v}\, I.Q.I^t e^{A^t.v}\, dv \approx T_s.I.Q.I^t \;\; if\; T_s < \tau \tag{22}$$

$$R_d = R/T_s \tag{23}$$

Where expressions of Q an R are given in detail in [23], τ is the response time of the system. A method is proposed here to dimension τ. It resides on choosing τ smaller than the smallest time constant of the SPSG (the electric time constant).Then, one has to calculate the armature and the field time constants ($\tau_{ea} = L_a/r_a\,, \tau_{ef} = L_f/r_f$) starting from the SI values of the self-inductances, and resistances identified by off-line tests recommended by the international standardization [9]. Since that the time-constants must be calculated in SI units.

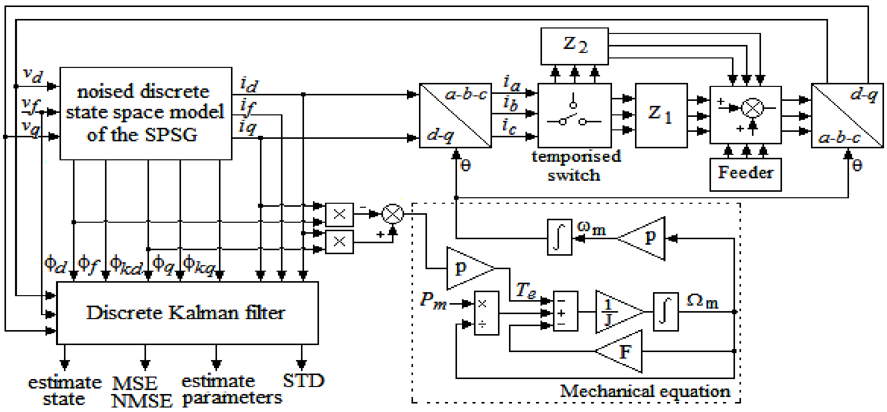

Fig.4. Depiction of the system under consideration

5.2. Application of the DTKF

Fig. 5 presents the theory and application of DKF, the flow chart of Fig.5.a inspired from [32] demonstrates the work which must be done to implement the DTKF. The work is based on two steps: the update and the prediction [31-33].

Update step

It consists of updating the measurement and the time as mentioned in (24)-(28) expressing respectively the Kalman filter gain, the estimated and predicted state variables, the error and predicted covariances according to the new measurement y(k).

$$K_f = P(k|k-1).C_d^t.(C_d.P(k|k-1).C_d^t + R_d)^{-1} \tag{24}$$

$$\hat{x}(k|k) = \hat{x}(k|k-1) + K_f.(y(k) - C_d.\hat{x}(k|k-1)) \tag{25}$$

$$\hat{x}(k+1|k) = A_d.\hat{x}(k|k) + B_d.u(k) \tag{26}$$

$$P(k|k) = \left(I - K_f.C_d\right).P(k|k-1) \tag{27}$$

$$P(k+1|k) = A_d.P(k|k).A_d^t + Q_d \tag{28}$$

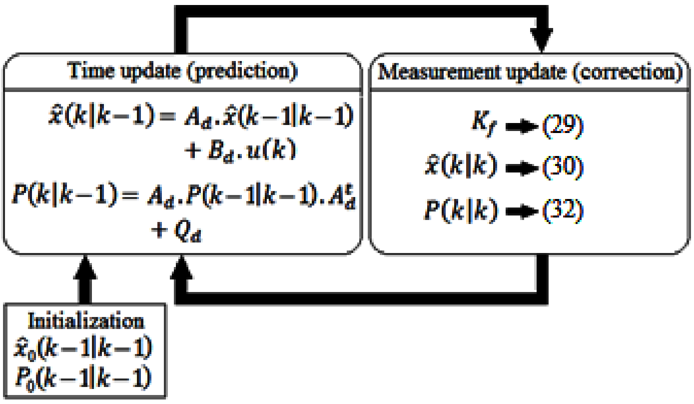

(a)

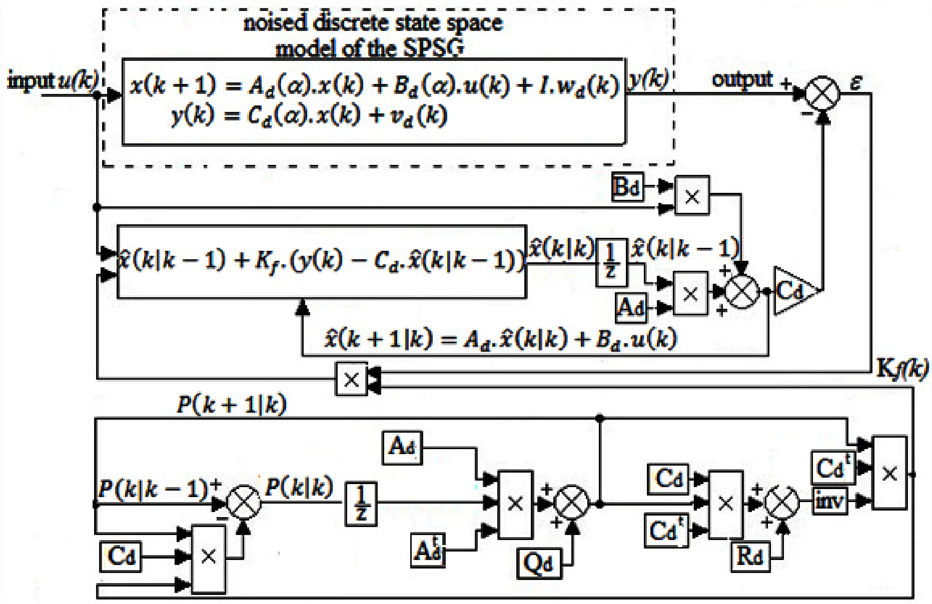

(b)

Fig.5. Theory of discrete Kalman Filter (a) Algorithm of DTKF (b) Principle of DTKF

Where $\hat{x}(k|k-1)$ is the estimate of $\hat{x}(k)$ given previous measurement $y(k-1)$ and $\hat{x}(k|k)$ is the updated estimate based on the last measurement $y(k)$.

Prediction step

Given the current estimate $\hat{x}(k|k)$, the time update predicts the state value at the next sample $k+1$ (one-step-ahead predictor). The measurement update then adjusts this prediction based on the new measurement $y(k+1)$. The correction term $(y(k+1) - C_d.\hat{x}(k+1|k))$ is a function of the innovation which is the discrepancy between the measured and the predicted values of $y(k+1)$. The innovation gain K_f is chosen to reduce the steady-state covariance of the estimation error given the noise covariances Q_d and R_d.

5.3. Application of the DEKF

The use of the DEKF is the best solution for time varying parameters [28]; consequently they should be treated as parameter states. As a result the system contains two state vectors 'x' and 'σ' grouped in a vector 'z' as mentioned in (29).

$$z = \begin{bmatrix} x \\ \sigma \end{bmatrix} \Rightarrow \dot{z} = \begin{bmatrix} f(\alpha, x(k), u(k)) \\ 0 \end{bmatrix} \tag{29}$$

The work to be done with the DEKF is quite similar to DTKF. Though, the calculation of the Kalman gain $K_f(k)$ and covariance matrix $P(k)$ is different. Indeed, this time, the Jacobian of matrices A_d and C_d *vs*. the estimated state variable and estimated parameters (noted A_{DEKF}, C_{DEKF}) has to be applied to calculate $K_f(k)$ and $P(k)$.

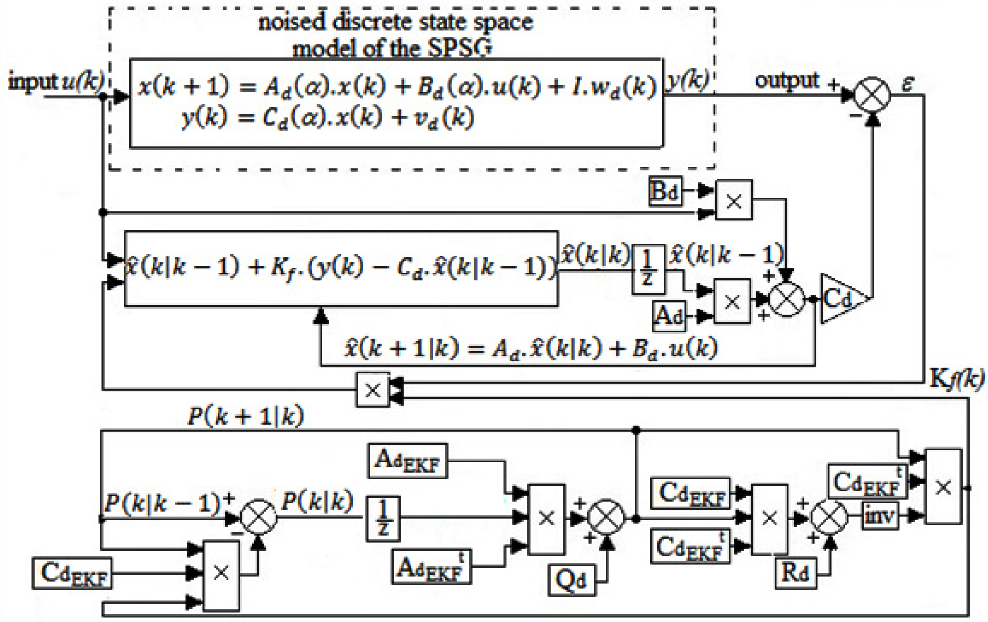

Fig.6. Chart of EKF principle

$$A_{dEKF} = Jacobian(\dot{z}, z) = \frac{\partial \dot{z}}{\partial z} \tag{30}$$

$$C_{dEKF} = Jacobian(y, z) = \frac{\partial y}{\partial z} \tag{31}$$

5.4. Application of the BEKF

The biased state variable is defined by [18]:

$$\hat{x}_b = b.\hat{x} \quad (32)$$

b is the bias coefficient which must be designed to reduce the MSE, *i. e.*:

$$MSE_{biased} < MSE_{unbiased} \quad (33)$$

Where

$$\mathrm{MSE_{biased}}(x, \hat{x}_b) = E(\hat{x}_b - x)^2 \quad (34)$$

$$E(\hat{x}_b - x)^2 = \frac{1}{L}.\sum_{i=1}^{L}(\hat{x}_{bi} - x_i)^2 \quad (35)$$

Then, the mathematical development of (35) gives:

$$E(\hat{x})^2.b^2 - 2.E(\hat{x}.x).b + E(x)^2 < trace(P)$$

All values inferior to $trace\,(P(k))$ and which carries out a positive real value of b that verifies (33) can be accepted. Let name these values 'c'. Then the resolve of the equation:

$$E(\hat{x})^2.b^2 - 2.E(\hat{x}.x).b + E(x)^2 - c = 0$$

Resulted in the smallest root:

$$b = \frac{2.E(\hat{x}.x) - \sqrt{\left(2.E(\hat{x}.x)\right)^2 - 4.E(\hat{x})^2.(E(x)^2 - c)}}{2.E(\hat{x})^2} \quad (36)$$

Finally, the $NMSE_{biased}$ is expressed by:

$$NMSE_{biased}(dB) = 20.log_{10}\left(\frac{MSE_{biased}(x,\hat{x}_b)}{E(x)^2}\right) \quad (37)$$

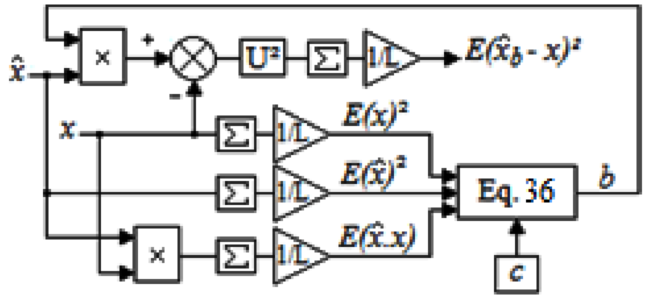

Fig.7. Principle of the proposed DBEKF

6. Methodology of parametric estimation

The estimated parameters gathered in vector σ can be obtained as follows:

6.1. The Steady State Estimated Parameters

The method of estimation consists in considering the set of equations from (1) to (10), and then the variable states are replaced by the estimated ones given by (25). Finally equations (1) to (10) are rewritten so that the unique unknowns are $\hat{r}_f, \hat{L}_{md}, \hat{L}_{mq}$, the other parameters are being replaced by their real values obtained via off-line method mentioned in section 2. Then the solution of equation (38) gives the steady state estimated parameters noted α_{ss}:

$$H_{ss}.\alpha_{ss} = G_{ss} \Rightarrow \alpha_{ss} = H_{ss}^{-1}.G_{ss} \quad (38)$$

Where

$\alpha_{ss} = [\hat{r}_f \hat{L}_{md} \hat{L}_{mq}]$,

$$H_{ss} = \begin{bmatrix} i_f & 0 & 0 \\ 0 & \omega_s/\omega_b . i_q & 0 \\ 0 & 0 & \omega_s/\omega_b . (i_f + i_d) \end{bmatrix},$$

$$G_{ss} = \begin{bmatrix} 1 & 0 & 0 \\ 0 & 1 & 0 \\ 0 & 0 & -1 \end{bmatrix} . \left(\begin{bmatrix} E_f \\ v_d \\ v_q \end{bmatrix} - \begin{bmatrix} d\hat{\phi}_f/dt \\ d\hat{\phi}_d/dt \\ d\hat{\phi}_q/dt \end{bmatrix} \right) - \left(\begin{bmatrix} 0 & 0 & 0 \\ 0 & r_a & 0 \\ 0 & 0 & -r_a \end{bmatrix} + \begin{bmatrix} 0 & 0 & 0 \\ 0 & 0 & \omega_s . l_a \\ 0 & \omega_s . l_a & 0 \end{bmatrix} \right) . \begin{bmatrix} \hat{i}_f \\ \hat{i}_d \\ \hat{i}_q \end{bmatrix} \quad (39)$$

6.2. The Transient State Estimated Parameters

Eq (40) gives the transient state estimated parameters α_{ts}:

$$H_{ts} . \alpha_{ts} = G_{ts} \Rightarrow \alpha_{ts} = H_{ts}^{-1} . G_{ts} \quad (40)$$

Where

$\alpha_{ts} = [\hat{l}_{kd} \hat{l}_{kq}]$,

$$H_{ts} = \begin{bmatrix} d\hat{\phi}_{kd}/dt & 0 \\ 0 & d\hat{\phi}_{kq}/dt \end{bmatrix},$$

$$G_{ts} = \begin{bmatrix} r_{kd} . \omega_b & 0 \\ 0 & r_{kq} . \omega_b \end{bmatrix} . \begin{bmatrix} \hat{\phi}_{kd} \\ \hat{\phi}_{kq} \end{bmatrix} + \begin{bmatrix} -r_{kd} . \omega_b . X_{md} & 0 \\ 0 & -r_{kq} . \omega_b . X_{mq} \end{bmatrix} . \begin{bmatrix} \hat{i}_d \\ \hat{i}_q \end{bmatrix} + \begin{bmatrix} -r_{kd} . \omega_b . X_{md} . \hat{i}_f \\ 0 \end{bmatrix} \quad (41)$$

7. Simulation results

Using the real parameters of the SPSG mentioned in Table 4, MATLAB codes and Simulink models were performed to implement the different DKFs discussed in this paper. The chosen value for the sample time is $T_s = 5\mu sec$. The noise state and measurement covariances are $Q = 1.4\, p.u.$ and $R = 10^{-5}\, p.u.$ Consequently, the discrete noise covariances equal to: $Q_d = Q \times T_s\, p.u.$ while$R_d = R/T_s\, p.u.$ to be entered as matrices of 5×5.

First of all, Fig. 8 and Fig. 9 show the d-q axis voltages and currents in p. u. note that a sudden change in the feeder impedance (from z1 to z2) is set at 0.25sec. The voltages and currents illustrate a satisfying p. u. value which demonstrates a normal behavior of the modeled SPSG, if compared with the results presented in [28] which consists of the basis reference in this study.

Fig. 10 shows that the estimated d-q axis fluxes obtained from both DTKF and DEKF estimators. One notices that estimated fluxes of both estimators have the same pace, meaning that both estimators have similar behavior.

Fig. 11 depicts the estimated parameters of the steady state $\hat{r}_f, \hat{L}_{md}, \hat{L}_{mq}$. The estimation process starts at 0.1 sec in order to meet the steady state (from 0 to 0.1sec the real value of the parameter is displayed). It's clear that the estimated parameters are close to the real parameters and the the EKF carries-out less noised parameters.

Fig.12 mentions the results of the transient state (the estimation process starts at 0.25sec coinciding with the feeder impedance variation), the concerned estimated parameters are dampers leakage inductances $\hat{l}_{kd}, \hat{l}_{kq}$. It can be conclude that DEKF gives quite better results than DTKF this time.

As it was concluded in the previous work [23,24] , it's obvious that the DEKF is more effective in the estimation as well as in filtering the noise effect, as it is shown in the Table 5 the STD issued by both estimators. The Table demonstrates the effectiveness of the DEKF which carried-out lesser STD compared to the DTKF.

Table 5: The standard deviation (STD) results

Real Parameter (p.u.)		STD DTKF (%)	STD DEKF (%)
r_f	0.334	0.0921	0.0692
L_{mq}	0.6637	1.0949	0.9302
L_{md}	1.351	1.5378	1.0292
l_{kd}	0.2026	0.7866	0.6888
l_{kq}	0.2471	3.8578	2.5664

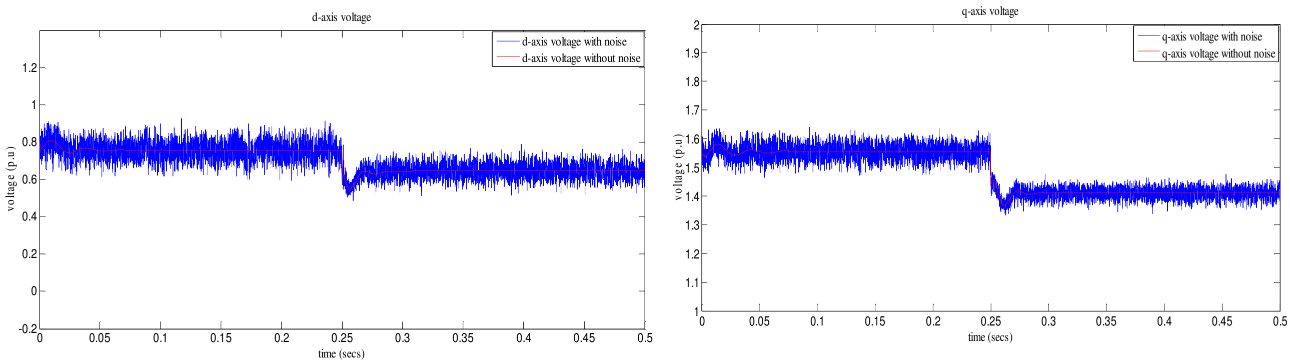

(a) (b)

Fig.8. d-q axis noised and non-noised voltages (a) d-axis voltage (b) q-axis voltage.

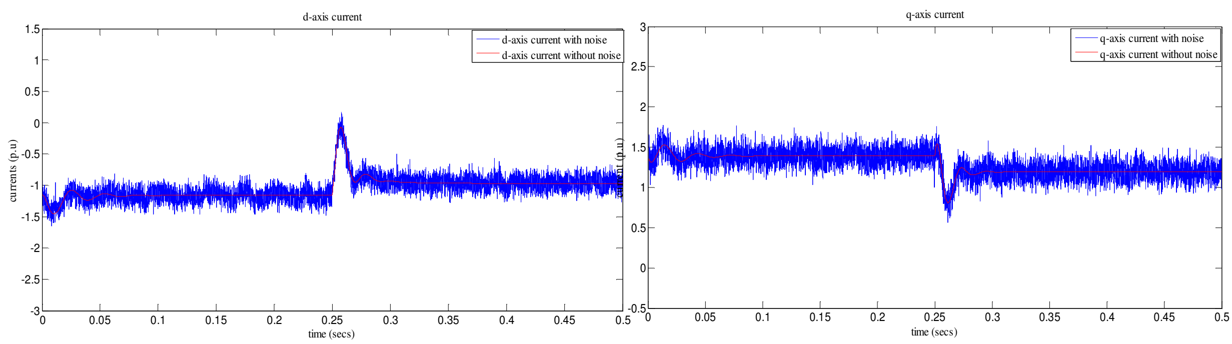

(a) (b)

Fig.9. d-q axis noised and non-noised currents (a) d-axis current (b) q-axis current.

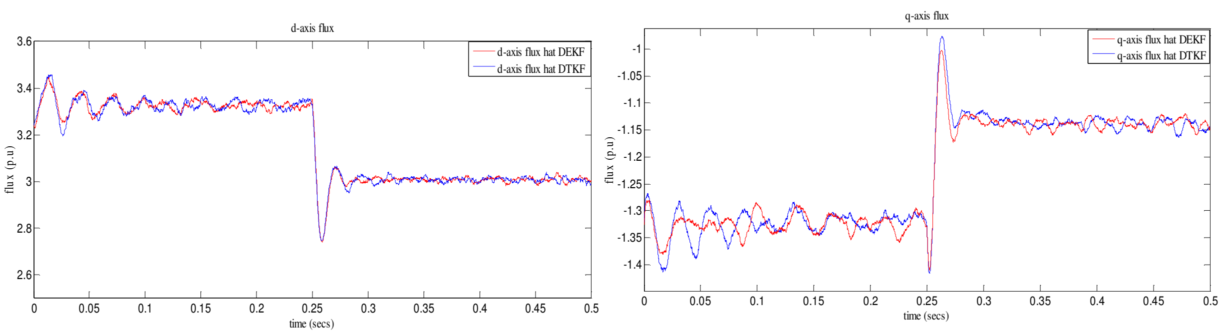

(a) (b)

Fig.10. d –q axis estimated fluxes obtained from DTKF and DEKF (a) d-axis current (b) q-axis current.

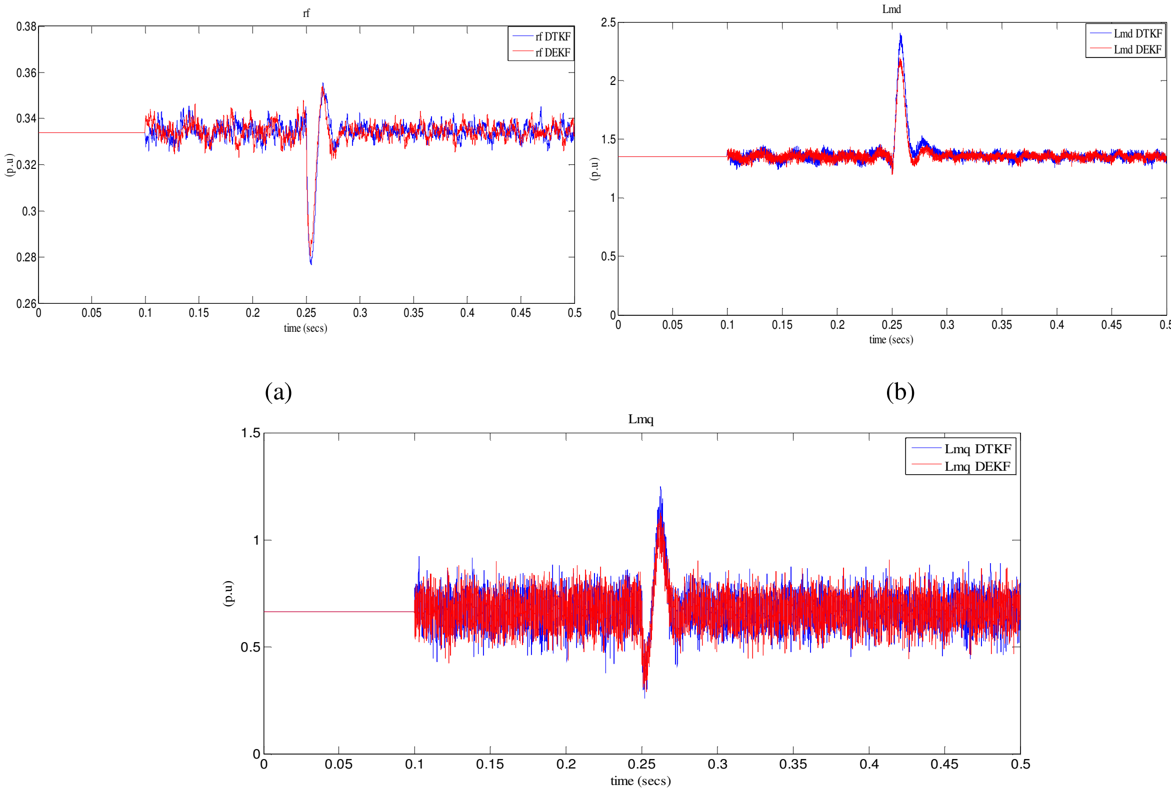

(a) (b)

(c)

Fig.11. Estimated parameters of the steady state (a) r_f (b) L_{md} (c) L_{mq}

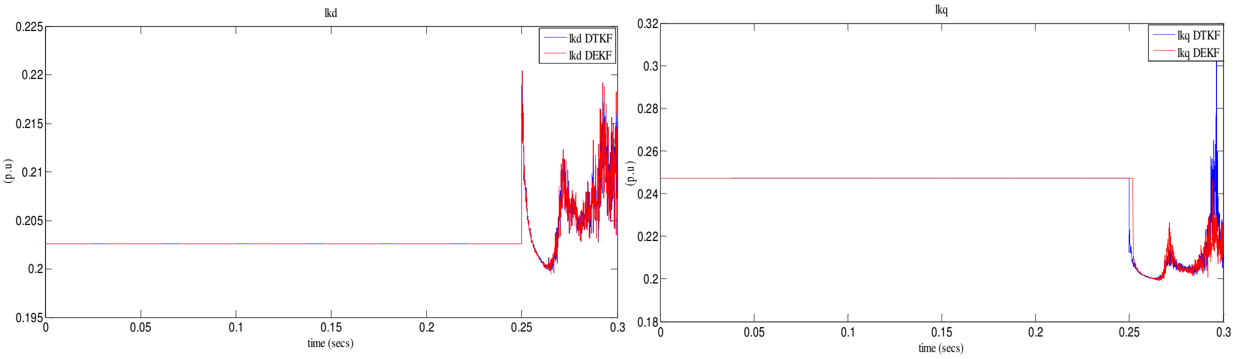

(a) (b)

Fig.12. Estimated parameters of the transient state (a) l_{kd} (b) l_{kq}.

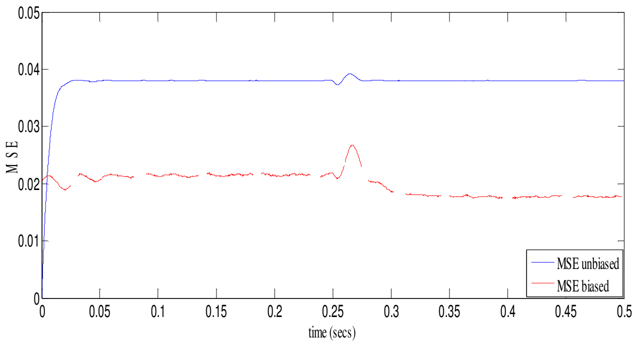

Fig.13. MSE of unbiaised and biaised DEKF.

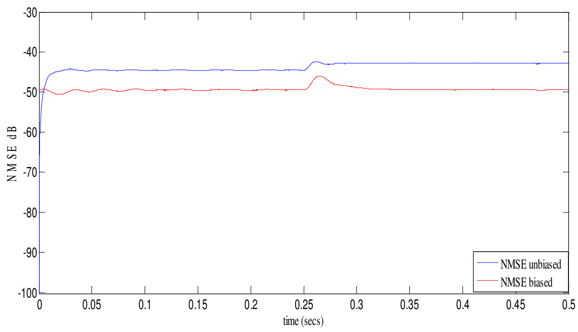

Fig.14. NMSE of unbiased and biased DEKF.

The study of MSE and NMSE were performed on the DEKF estimator giving better estimation quality as previously mentioned. Results are reported in Fig.13 and 14.
Fig.13 demonstrates a less MSE obtained in the case of considering the bias. In fact $MSE_{unbiased} \approx 0.0381$, $MSE_{biased} = 0.0201$ where c =0.02 which gave b = 0.942; Consequently the NMSE is smaller as shown in Fig.14 , $NMSE_{biaised} \approx 48.58$ dB, $NMSE_{unbiaised} = -42.89$dB.

8. Conclusions

Off-line methods founded on stand-still tests can't be accurate to identify the parameters of SPSG's since those parameters maintain changements during on-line operating. Therefore, on-line parametric estimation is essential to output more accurate estimates following the continuous variations provided that external data about voltages, currents and rotor position are unceasingly available. This study aims at performing an on-line parametric estimation on a very low scale SPSG by a varing impedance feeder.
An earlier work [25] was dedicated to extract the real parameters values on the basis of off-line standstill tests [4,8,9]. The next works established on the SPSG considered [28] were accomplished in order to compare between continous, and discrete Kalman Filters parametric estimation where the comparison favorised the discrete KF giving better results which justifies its use in this study.
The presented results show satisfying p.u. values for d-q voltages and currents of the SPSG. Moreover, the displayed curves of the steady and transients states parameters as well as data recorded in table 5 and the MSE/NMSE plots demontrated the effectiveness of the biaised DEKF estimator compared with the other studies estimators.
The prospective work is concerned with the practical analysis of the presented study. The experimental setup is already operational and the results are being extracted using a DSPACE 1104 chip board interface.

References

[1] P. L. Dandeno, Current usage & suggested practices in power system stability simulations for synchronous machines, *IEEE Transactions on Power Conversion*, 77-93, 1986.

[2] Z. Zhao, F. Zheng & L. Xu, A dynamic on-line parameter identificationand full-scale system experimental verification for large scale synchronous machines, *IEEE Transaction on Energy Conversion*, *10(3),*392-398, 1995.

[3] L. Xu, Z. Zhao & J. Jiang, On-line estimation of variable parameters of synchronous machines using a novel adaptive algorithm - Estiùation and experimental verification , *IEEE Transaction on Energy Conversion*, *12(3),* 200-210, 1997.

[4] IEEE Std.115A-1987, IEEE standard procedures for obtaining synchronous machine parameters by standstill frequency response testing , Supplement to ANSI/IEEE Std. 115A-1983.

[5] R. K. Nezhad, R.Hooshmand, M. P. Moghaddam & G. A. Montazer, Synchronous generator parameter estimation by genetic algorithms, AUPEC 2002, Melbourn, Australia, Sept., 29th-Oct. 2nd, 2002.

[6] M. Hasni , Synchronous machine parameter identification in frequency and time domains, *Serbian Journal of Electrical Engineering*, *4(1),* 51-69, 2007.

[7] P. J. Turner, A. B. J. Reece & D. C. Macdonald, The DC decay test for determining synchronous machines parameters: Measurment and simulation, *IEEE Power Engineering Review,*1989.

[8] J. Lesenne, F. Notelet & G. Seguier, Introduction a l'electrotechnique approfondie , *Technique & documentation*, Paris, 1981.

[9] Int. Std. IEC, Rotating electrical machines– Part 4: Methodes for determining synchronous machine quantities from tests, IEC60034-4,2008.

[10] H. B. Karataka , Synchronous generator model identification and parameter estimation from operating data, *IEEE Transaction on Energy Conversion*, *18(1),* 121-126, 2003.

[11] T. Boileau , On-line identification of PMSM parameters: Parameter identifiability and estimator comparative study, *IEEE Transaction on Ind. Applic.*, *47(4),*1944-1957, 2011.

[12] D. Simon, Kalman filtering with state constraints: a survey of linear and nonlinear algorithms, *Control Theory & Applications*, *IET*, *4(8),* 1303-1318, 2010.

[13] Lingling Fan**,** ''Least Squares Estimation and Kalman Filter Based Dynamic State and Parameter Estimation'' 978-1-4673-8040-9/2015 IEEE.

[14] K. Reif & R. Unbehauen, The extended Kalman filter as an exponential observer for nonlinear systems, *IEEE Transaction on Signal Processing*, *47(8),* 2324-2328, 1999.

[15] E. A. & Wan R.Van Der Merwe, The unscented Kalman filter for nonlinear estimation, *IEEE Symposium Adaptive Systems for Signal Processing*, *Communications and Control*, 153-158, Lake Louise, Alta, 2000.

[16] Hossein Ghassempour Aghamolki, Zhixin Miao, Lingling Fan, Weiqing Jiang,Durgesh Manjure''Identification of synchronous generator model with frequency controlusing unscented Kalman filter'' *Electric Power Systems Research* 126,45–55, 2015 Elsevier.

[17] S. Mejri, A. S. Tlili & N. B. Braiek, On the state estimation of chaotic systems by a particle filter and an extended Kalmanfilter, *11th International Multi-Conference on Systems, Signals & Devices,* Barcelona, 2014.

[18] T. Jiajia,D. Li, J. Q. Zhang, B. Hu & Q. Lu, Biased Kalman filter, *5th International Conference on Sensing Technology*, 581-584, PalmerstonNorth, 2011.

[19] S. Kluge, K. Reif, M. Brokate, "Stochastic Stability of the Extended Kalman Filter With Intermittent Observations," *IEEE Trans. on Automatic Control,* 55 (2) , 514-518, Feb. 2010.

[20] J. E. Bester, A. E. Hajjaji, A. M. Mabwe, "Modelling of Lithium-ion battery and SOC estimation using simple and extended discrete Kalman Filters for Aircraft energy management,"IECON 2015, Yokohama, 9-12 Nov. 2015.

[21] Hyun-Woo Sim, June-Seok Lee and Kyo-Beum Lee ,''On-line Parameter Estimation of Interior Permanent Magnet Synchronous Motor using an Extended Kalman Filter'' J Electr Eng Technol 9(2) : 600-608, 2014.

[22] R. Feynman, Discrete-Time System Properties, web site: http://highered.mheducation.com/sites/dl/free/0073404543/367604/Roberts_ch5.pdf.

[23] M. Larakeb, A. Bentounsi & H. Djeghloud, Biased Kalman filter applied for on-line estimation of SPSG parameters, *5th Intern. Conf. on Systems and Control (ICSC'16)*, Marrakech, 2016.

[24] M. Larakeb, A. Bentounsi & H. Djeghloud, On-line estimation of SPSG parameters using discrete kalman filter, *17th Intern. Conf. on Enviromment and Electrical Engineering (IEEE)*, Florence, 2016.

[25] H. Djeghloud, A. Bentounsi & M. Larakeb, Real and virtual labs for enhancing an SM course , *15th Intern. Conf. on Electrcial Machines and Systems (ICEMS 2012)*, Sapporo, Japan, 2012.

[26] H. Djeghloud, M. Larakeb & A. Bentounsi, Virtual labs of conventional electric machine, *15th Intern. Conf. on Electrcial Machines and Systems (ICEMS 2012),* Sapporo, Japan, 2011.

[27] J. Chatelain, Machines électriques, English version : Electrical machines, *Chapter 7*, 345-346, *Ed. Dunod* 1983, *Presses polytechniques romandes*.

[28] R. E. Fairbain & R. G. Harley, On-line Measurement of synchronous Machine Parameters, *IEEE Transaction on Ind. Applic.*,*28(3),* 1992.

[29] E. Kyriakides, G. T. Heydt & V. Vittal, On-line estimation of synchronous generator parameters using a damper current observer and graphic user interface, *IEEE Transaction on Energy Conversion*, *19(3),* 499-507, 2004.

[30] M. Salgado, R. Middleton & G.C. Goodwin, Connection between continuous and discrete Riccati equations with applications to Kalmanfiltering, *IEE Proceding* ,135(1), 28-34,1988.

[31] D. Alazar, Introduction au filtre de Kalman, English version : Introfvution to the Kalman filter*, Lecture Notes*, 1-73, 2006.

[32] G. Welch & G. Bishop, An Introduction to the Kalman Filter, *University of North Carolina at Chapel Hill, Department of Computer Science*, TR 95-041, 2006.

[33] M.J.Grimble, Robust Industrial Control: Optimal Design Approach for Polynomial Systems, *Prentice Hall*, 443-456, 1994.